Viscous Dissipation Effect in Trapezoidal Microchannels at Constant Heat Flux

Talie SHEIKHALIPOUR [1], Abbas ABBASSI [1,*]

* Corresponding author: Tel.: ++98 (21)64543425; Fax: ++98 (21)66619736; Email: abbassi@aut.ac.ir
1: Amirkabir University of Technology, Mechanical Engineering Department, Tehran, Iran

Abstract: Present paper is dealt with the steady state, laminar and hydrodynamically and thermally developed flow in a trapezoidal channel under H2 boundary condition is investigated. Slip flow, temperature jump and viscous dissipation effects are considered. Firstly, Navier-Stokes equations are transformed from physical plane to square domain, and then solved using finite difference method. Also, it is possible to obtain fluid flow and heat transfer characteristics for a rectangular microchannel with this method. The effects of aspect ratio, rarefaction, base angle and viscous heating on Nusselt number are discussed. The results of the numerical method are verified with the conventional theory of macrochannels (i.e. Kn=0, Br=0). Also, the friction factors and the Nusselt numbers for Br=0, Kn≠0 are in a good agreement with the available results of flow and heat transfer of rectangular microchannels in the literature. The results showed that the increase in rarefaction reduces the Nusselt numbers in trapezoidal and rectangular microchannels. When the *Kn* number is fixed and the *Br* number is small, the microchannel with the higher aspect ratio has the greater *Nu*, but for higher *Br* numbers, the greater aspect ratio results in smaller *Nu*. Also, at the same rarefaction, when *Br* number is large, the difference between *Nu* number of different aspect ratios decreases.

Keywords: microchannels, viscous dissipation, trapezoidal, H2 boundary condition

1. Introduction

Flow and heat transfer in microchannels has been studied by many researchers in recent years, but the literature still is open. The need for efficient cooling in micro devices has led to more investigation about cooling features of microchannels. A great amount of work has been put into development of components such as micropump, microvalves, mixing chambers. Microfluidic devices are already at a stage where further development requires the use of simulation capabilities.

Tunc [1] studied the convective heat transfer for steady state, hydrodynamically developed laminar flow in micro tubes with uniform temperature and uniform heat flux boundary conditions by integral transform technique. Temperature jump at the wall and viscous heating within the medium were included. The effect of viscous heating was investigated for both of the cases where the fluid was being heated or cooled. They showed that the viscous heating has different effects for different cases. Barron et al [2] extended the original Graetz problem for thermally developing heat transfer in laminar flow through circular tube to include the effects of slip-flow. He suggested that slip-flow is one of the mechanisms being responsible for the enhancement of the heat transfer in gaseous convection in micro tubes. Bayazitoglu and Kakac [3] discussed the flow field in microchannel single phase gaseous fluid flow. They noted that viscous heating, compressibility and rarefaction is to be considered in gaseous flows in microchannels. Koo and Kleinstreuer investigated the viscous dissipation effects on the temperature field and friction factor in circular and rectangular microchannels [4]. They demonstrated that viscous dissipation is a strong function of the hydraulic diameter, the channel aspect ratio, and the Brinkman number. Also, a numerical analysis of slip velocity and temperature jump effects on friction factor and Nusselt number

has been studied numerically by Cao et al. [5]. Morini [6] studied the role of viscous heating in liquid flows in microchannels. A model based on the conventional theory was developed to predict the viscous dissipation effects with the same method, Kuddusi and Cetegen analyzed thermal and hydrodynamic characteristics of a hydrodynamically developed and thermally developing flow in trapezoidal silicon microchannels [7]. Among non-circular cross section microchannels, those with trapezoidal and rectangular cross section shapes are more used. It is seen that there is a lack of researches to consider the effects of viscous dissipation in gas flow in non-circular microchannels in the literature.

Different phenomena have been observed in various works indicating that the mechanisms of flow and heat transfer in microchannels are not understood clearly yet. It seems reasonable to say that, the Knudsen number *Kn* can categorize the gas flow in channels into four regimes: continuum flow (Kn<0.001), slip flow (0.001<Kn<0.1), transition (0.1<Kn<10), and free molecular flow regime (Kn>10). Though the numerical results of this paper is obtained for the slip flow regime (i.e. 0.001<Kn<0.1), this analysis is not secure near Kn=0.1 and is away from the real results. There are some articles available in the literatures that have solved the flow in the transition regime using Boltzmann equation, which are more reliable [8, 9]. It must be taken into consideration that viscous dissipation effect is not included in their results.

In the present work, convective heat transfer in trapezoidal microchannels is numerically investigated. The flow is assumed steady, laminar and hydrodynamically and thermally developed, slip flow, temperature jump and viscous dissipation effects are considered. It is assumed that the heat flux is constant (H2 boundary condition).

2. Governing Equations

A trapezoidal microchannel is considered under steady laminar incompressible flow. Also, it is assumed that the fluid is Newtonian. Slip flow and temperature jump at the walls is considered. Figure 1 shows the geometry of the microchannel.

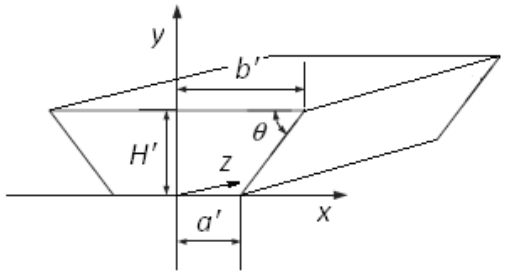

Figure 1: The geometry of microchannel.

The z-momentum equation for a hydronamically developed flow can be written as:

$$\frac{\partial^2 u}{\partial x^2}+\frac{\partial^2 u}{\partial y^2}=\frac{1}{\mu}\frac{\partial P}{\partial z} \tag{1}$$

And the energy equation with considering the viscous dissipation effect is as follows:

$$k\left(\frac{\partial^2 T}{\partial x^2}+\frac{\partial^2 T}{\partial y^2}\right)+\mu\left(\left(\frac{\partial u}{\partial x}\right)^2+\left(\frac{\partial u}{\partial y}\right)^2\right)=\rho C_p u\frac{\partial T}{\partial z} \tag{2}$$

For the thermally developed region and H1 boundary condition,

$$\frac{\partial T}{\partial z}=\frac{\partial T_m}{\partial z} \tag{3}$$

Where T_m is the mean temperature of the cross-section and is defined as:

$$T_m=\frac{1}{\rho C_p u_m A_c}\iint_{A_c}\rho C_p u T dA_c \tag{4}$$

The energy balance equation gives the axial variation of bulk temperature:

$$\frac{\partial T_m}{\partial z}=\frac{q''p+\int_{A_c}(\nabla u.\nabla u)dA_c}{\rho C_p u_m A_c} \tag{5}$$

u_m is the mean velocity in the cross-section:

$$u_m=\frac{1}{A_c}\iint_{A_c} u dA_c \tag{6}$$

2.1 Velocity Slip and Temperature Jump Boundary Conditions

To obtain the solution of the mentioned governing equations, fluid velocity and

thermal conditions at the boundaries must be specified. In the slip region, the velocity does not vanish at the stationary surfaces and the fluid temperature near the wall is not the same as the surface. The following equations are an approximation for velocity slip and temperature jump boundary conditions [2]:

$$u_s - u_w = \beta_v Kn \frac{\partial u}{\partial n}|_{wall} \quad (7)$$

$$T_s - T_w = \beta_T Kn \frac{\partial T}{\partial n}|_{wall} \quad (8)$$

Where

$$\beta_v = \frac{2-\sigma_v}{\sigma_v} \quad , \quad \beta_T = \frac{2-\sigma_T}{\sigma_T}\frac{2R}{R+1}\frac{1}{\Pr} \quad (9)$$

And H2 boundary condition is:

$$-k\frac{\partial T}{\partial n}|_{wall} = q'' \quad (10)$$

Whereas R represents the specific heat ratio and Pr is the Prandtl number which is defined as $\Pr = \nu/\alpha$. The coefficients σ_v and σ_T are tangential momentum accommodation and thermal accommodation coefficient, respectively. Depending on the fluid, the solid and the surface finish these coefficients vary from 0 to 1.

2.2 Dimensionless Equations

By introducing the following non-dimensional coordinates,

$$\tilde{x} = x/D_h, \quad \tilde{y} = y/D_h, \quad \tilde{z} = \frac{z}{D_h \operatorname{Re}\Pr} \quad (11)$$

And the dimensionless temperature,

$$\theta = \frac{T - T_{in}}{q'' D_h / k} \quad (12)$$

(1) and (2) can be written as:

$$\frac{\partial^2 V}{\partial \tilde{x}^2} + \frac{\partial^2 V}{\partial \tilde{y}^2} = \frac{D_h^2}{u_m \mu}\frac{\partial P}{\partial z} \quad (13)$$

$$V\frac{\partial \theta}{\partial \tilde{z}} = \frac{\partial^2 \theta}{\partial \tilde{x}^2} + \frac{\partial^2 \theta}{\partial \tilde{y}^2} + Br\left((\frac{\partial V}{\partial \tilde{x}})^2 + (\frac{\partial V}{\partial \tilde{y}})^2\right) \quad (14)$$

Where, V is the dimensionless velocity, Re and Br are Reynolds and Brinkman number respectively and are defined as follows:

$$V = \frac{u}{u_m}, \quad \operatorname{Re} = \frac{u_m D_h}{\upsilon}, \quad Br = \frac{\mu u_m^2}{q'' D_h} \quad (15)$$

Thus,

$$\frac{\partial \theta_m}{\partial \tilde{z}} = 4(1 + Br\Phi^* D_h / p) \quad (16)$$

Φ^* is the non-dimensional viscous dissipation and is obtained from the following equation [10]:

$$\Phi^* = 2(A_c / D_h^2) f \operatorname{Re} \quad (17)$$

So, the equation (13) becomes

$$4(1 + Br\Phi^* / p^*) = \frac{\partial^2 \theta}{\partial \tilde{x}^2} + \frac{\partial^2 \theta}{\partial \tilde{y}^2} + Br\left((\frac{\partial V}{\partial \tilde{x}})^2 + (\frac{\partial V}{\partial \tilde{y}})^2\right) \quad (18)$$

Where p^* is the dimensionless perimeter of the microchannel ($p^* = p/D_h$).

With dimensionless boundary conditions:

$$V_s = \beta_v Kn \frac{\partial V}{\partial \tilde{n}}|_{wall} \quad (19)$$

$$\theta_s - \theta_w = \beta_T Kn \frac{\partial \theta}{\partial \tilde{n}}|_{wall} = -\beta_T Kn \quad (20)$$

2.3 Coordinate Transformation

The governing equations are transformed from physical plane to the square domain as shown in Figure 2:

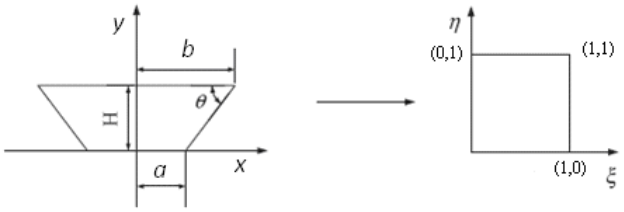

Figure 2: The non-dimensional domain and the transformed square.

By applying the following equations, the new independent variables in the square domain will be obtained:

$$\xi = \frac{(a+x)H + (b-a)y}{2((b-a)y + aH)} \quad (21)$$

$$\eta = y/H \quad (22)$$

So, the governing equations in the transformed domain are written as:

$$\frac{\partial^2 \phi}{\partial \tilde{x}^2} + \frac{\partial^2 \phi}{\partial \tilde{y}^2} = C_1\frac{\partial^2 \phi}{\partial \xi^2} + C_2\frac{\partial^2 \phi}{\partial \eta^2} + C_3\frac{\partial^2 \phi}{\partial \xi \partial \eta} + C_4\frac{\partial \phi}{\partial \xi} + C_5\frac{\partial \phi}{\partial \eta} \quad (23)$$

, C_1, C_2, C_3, C_4 and C_5 are coefficients and J is the Jacobian of transformation:

$$J = x_\xi y_\eta - y_\xi x_\eta \tag{24}$$

$$C_1 = (x_\eta^2 + y_\eta^2)/J^2, C_2 = (x_\xi^2 + y_\xi^2)/J^2$$
$$C_3 = -2(x_\xi x_\eta + y_\xi y_\eta)/J^2, C_4 = \xi_{yy}, C_5 = 0 \tag{25}$$

The local normal gradient at the boundaries of computational domain is [11]:

$$\frac{\partial \phi}{\partial \tilde{n}^{(\eta)}} = \frac{(x_\xi^2 + y_\xi^2)\phi_\eta - (x_\xi x_\eta + y_\xi y_\eta)\phi_\xi}{J\sqrt{(x_\xi^2 + y_\xi^2)}},$$
$$\frac{\partial \phi}{\partial \tilde{n}^{(\xi)}} = \frac{(x_\eta^2 + y_\eta^2)\phi_\xi - (x_\xi x_\eta + y_\xi y_\eta)\phi_\eta}{J\sqrt{(x_\eta^2 + y_\eta^2)}} \tag{26}$$

The mean flow velocity and temperature in the cross-section are

$$u_m = \frac{\iint u J d\xi d\eta}{\iint J d\xi d\eta} \tag{27}$$

$$\theta_m = \frac{\iint \theta u J d\xi d\eta}{\iint u J d\xi d\eta} \tag{28}$$

And the Poiseuille number is obtained from:

$$f\,\mathrm{Re} = -\frac{D_h^2 \partial P/\partial z}{2\mu u_m} \tag{29}$$

The Nusselt number is defined as:

$$Nu = \frac{hD_h}{k} \tag{30}$$

Thus, with the definition of non-dimensional temperature, the Nusselt number can be written as follows:

$$Nu = \frac{1}{\theta_w - \theta_m} \tag{31}$$

3. Numerical Analysis

To discretize the governing equations a finite difference scheme is applied. Also, central difference is used to give more accurate solution. In the boundaries, the discretization is adopted so the accuracy remains second order. Grid independency is checked for more accuracy and a square grid with 50×50 nodes is used. The algebraic equations were solved by using of successive over-relaxation method. The iteration is terminated when the relative error reduces less than 10^{-6}. First, the momentum equation was solved and the velocity field and Poiseuille number obtained. Then, to determine the temperature distribution and Nusselt number, the energy equation was solved.

4. Results and discussion

To calculate the effect of aspect ratio, Br, and Kn numbers on friction factor and Nu number of a fully developed flow through a trapezoidal microchannel a computer code is written. It is also possible to use this procedure to obtain hydrodynamic and thermal features of a rectangular microchannel. The numerical calculations are carried out for Pr = 0.7, R = 1.4, σ_v = 1 and σ_T = 1. In this paper, the base angle of the trapezoid is equal to 54.74º, unless another condition is mentioned. This base angle is due to a common manufacturing method of silicon microchannels [10].

Table 1: The effect of rarefaction $\beta_v Kn$ on friction factor reduction, Φ, for different aspect ratios of rectangular and trapezoidal microchannels

	γ	Φ					
		0.01		0.05		0.1	
		Present Work	Morini [12]	Present Work	Morini [12]	Present Work	Morini [12]
Rect.	0.4	0.91889	0.917	0.695776	0.690	0.535696	0.529
	0.6	0.924861	0.923	0.714106	0.707	0.558073	0.551
	1	0.928682	0.926	0.725167	0.719	0.571971	0.565
Trap.	0.5	0.919673	0.918	0.693320	0.693	0.560413	0.532
	1	0.926298	0.924	0.719272	0.712	0.574955	0.555
	2	0.927285	0.926	0.721702	0.717	0.575467	0.562

Table 1 shows the effects of rarefaction on the Poiseuille number fRe for different aspect ratios for rectangular and trapezoidal microchannels. The aspect ratio γ is defined as H/(2×a). H is the height of microchannel and a is the half of minimum width of the cross-section as shown in Figure 2. Friction factor reduction, Φ, compares the Poiseuille number for an assigned value of the modified Knudsen number $\beta_v Kn$ with the value of the Poiseuille number when $\beta_v Kn$ = 0. For fixed aspect ratio, fRe decreases with the increase in $\beta_v Kn$. Also, the increase in aspect ratio results in reduction of the Nu number.

The results of the present work are compared with those of Morini et al. [12]. As

seen, the present results are in good agreement in these tables. This comparison verifies the reliability of the numerical calculation of the momentum equation.

Another comparison is made for the energy equation solution verification and is shown in Table 2. Kuddusi and Cetegen [13] derived the velocity and temperature distributions and thus, the average Nusselt number of a rectangular microchannel.

Table 2: The effect of rarefaction $\beta_v Kn$ on *Nu* for different aspect ratios of a rectangular microchannel

Kuddusi & Cetegen [7]

	aspect ratio				
Kn	1	0.8	0.6	0.4	0.2
0	3.093	3.0844	3.0522	2.9906	2.9249
0.02	2.9501	2.9546	2.9444	2.918	2.8962
0.04	2.774	2.7834	2.784	2.7755	2.7745
0.06	2.5912	2.6019	2.6074	2.6077	2.6156
0.08	2.4148	2.4254	2.4326	2.437	2.4481
0.1	2.2509	2.2606	2.2682	2.2741	2.2857

This Work

	aspect ratio				
Kn	1	0.8	0.6	0.4	0.2
0	3.0954	3.0854	3.0531	2.9993	2.9369
0.02	2.9876	2.9776	2.9445	2.8868	2.8072
0.04	2.8328	2.8313	2.7991	2.7402	2.6501
0.06	2.6744	2.6728	2.6425	2.5848	2.4900
0.08	2.5170	2.5154	2.4876	2.4327	2.3373
0.1	2.3672	2.3655	2.3403	2.2891	2.1959

The results of *Nu* number versus $\beta_v Kn$ for different base angles are shown in Figure 3. The results well agrees with the solution of $Kn = 0$ of [10]. As expected, the rarefaction has a decreasing effect on the value of the *Nu* number, but its reduction strongly depends on the microchannel base angle, and the effect of *Kn* number on the rectangular microchannel is the most.

The results of *Nu* number versus *Br* number for different *Kn* numbers are shown in Figure 4 for $\gamma = 0.5$ and 1 of a rectangular microchannel. Also the results of [8] agrees with the solution of $Kn = 0$. As expected, the rarefaction has a decreasing effect on the value of the *Nu* number.

At the same *Kn* number, when the *Br* number is small, the microchannel with the greater aspect ratio has a higher *Nu*, but when *Br* number increases, this conclusion is no longer valid. It seems that near $Br = 0.1$, the *Nu* number does not depend on the value of *Kn* number and the aspect ratio.

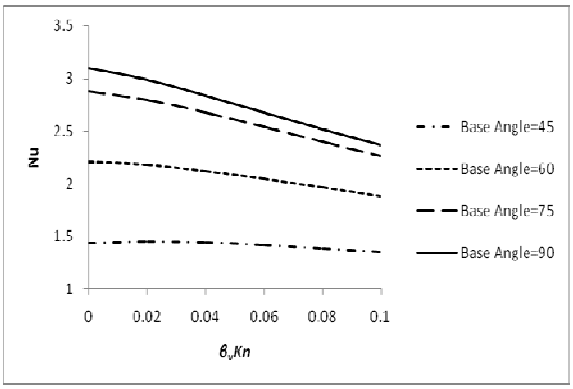

Figure 3: Variation of the *Nu* number with $\beta_v Kn$ of microchannels with different base angles, $\gamma = 1$.

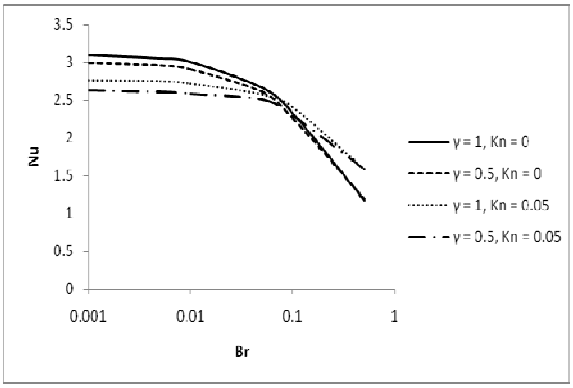

Figure 4: The effect of viscous dissipation on the *Nu* number for different $\beta_v Kn$ and aspect ratios for a rectangular microchannel.

Figure 5 shows the effect of viscous dissipation on the Nusselt number of a trapezoidal microchannel ($\theta = 75^\circ$, $\gamma = 1$). When the *Br* number is small, the *Nu* number decreases linearly with $\beta_v Kn$, but when viscous dissipation increases, it first increases slightly with rarefaction, and then decreases.

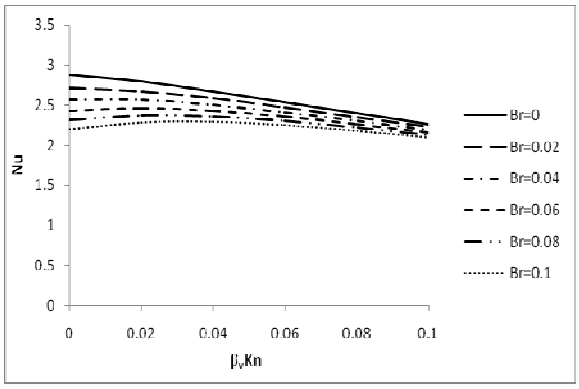

Figure 5: Variation of the *Nu* number with $\beta_v Kn$ of microchannels with different *Br* numbers, $\gamma = 1$, $\theta = 75^\circ$.

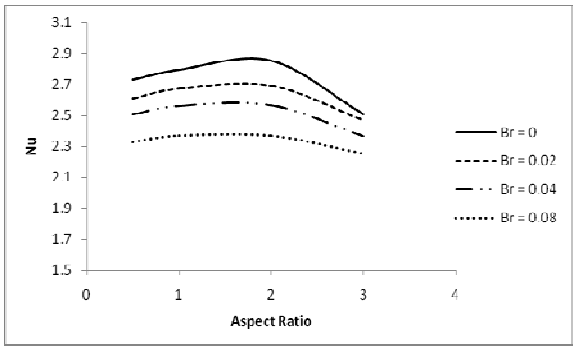

Figure 6: The *Nu* number versus aspect ratio for $\beta_v Kn$ = 0.02 and different *Br* for a trapezoidal microchannel, $\theta = 75^\circ$.

The effect of Nusselt number vs. aspect ratio is shown in Figure 6. The maximum *Nu* number occurs near $\gamma = 2$. In this vicinity, the increase of *Nu* is more when *Br* is smaller.

5. Conclusions

Fully developed laminar flow and heat transfer in trapezoidal microchannel is numerically investigated. Slip velocity and temperature jump condition at the walls is applied to obtain the characteristics of flow in the trapezoidal microchannel. H2 boundary condition is considered and finite difference scheme is applied for the solution of the problem. The transformation of trapezoidal geometry to a square makes it easy to generate uniform mesh in the computational domain. At the end, it can be concluded that:

1- The increase in rarefaction reduces the Nusselt numbers in trapezoidal and rectangular microchannels. Near Br = 0.1, the Nu numbers of microchannels with different Kn numbers converge to each other.

2- When the Kn number is fixed and the Br number is small, the microchannel with the higher aspect ratio has the greater Nu, but for higher Br numbers, the greater aspect ratio results in smaller Nu.

3- When the *Br* number is small, the *Nu* number reduces linearly with $\beta_v Kn$. Increase of viscous dissipation results in nonlinearity.

4- When the Br number is large, the difference between Nusselt numbers of a trapezoidal microchannel with different aspect ratios reduces.

Nomenclature

a	non-dimensional short base of microchannel
a'	short base of microchannel, m
A	area, m^2
b	non-dimensional long base of microchannel
b'	long base of microchannel, m
Br	Brinkman number
C_p	fluid specific heat, J kg^{-1} K^{-1}
D_h	hydraulic diameter of the duct, m
fRe	Poiseuille number
h	convective heat transfer coefficient, Wm^{-2} K^{-1}
H	non-dimensional height of microchannel
H'	height of microchannel, m
J	Jacobian
k	thermal conductivity of fluid, W m^{-1} K^{-1}
Kn	Knudsen number
n	normal to the inside of boundaries
Nu	Nusselt number
p	perimeter of the microchannel
P	pressure of the fluid in the duct, Pa
Pr	Prandtl number
Re	Reynolds number
T	fluid temperature, K
u	axial fluid velocity, m s^{-1}
V	dimensionless axial velocity defined by Eq.

14

x, y, z Cartesian coordinates

$\tilde{x}, \tilde{y}, \tilde{z}$ non-dimensional coordinates

Greek Symbols

α thermal diffusivity, $m^2 s^{-1}$

β dimensionless variable

γ aspect ratio

θ dimensionless temperature defined by Eq. 11

θ base angle, deg.

μ dynamic viscosity, kg $m^{-1} s^{-1}$

ν kinematic viscosity, $m^2 s^{-1}$

ρ fluid density, kg m^{-3}

σ_v thermal accommodation coefficient

σ_T tangential momentum accommodation coefficient

Φ friction factor reduction

Φ^* dimensionless viscous dissipation function defined by Eq. 16

ξ, η transformed coordinates

Subscripts

c cross-section

m mean value

s fluid property near the wall

w wall

References

[1] Tunc, G., & Bayazitoglu, Y. (2001). Heat transfer in micro tubes with viscous dissipation. *Int. J. Heat Mass Transfer*, **44**, 2395–2403.

[2] Barron, R. F., Wang, X. M., Warrington, R. O., & Ameel, T. A. (1997). The Graetz problem extended to slip flow. *Int. J. Heat Mass Transfer*, **40**, 1817–1823.

[3] Bayazitoglu, Y., & Kakac, S. (2005). Flow regimes in microchannel single phase gaseous fluid flow. *Microscale Heat Transfer- Fundamentals and Applications,* (edits) Kakac, S.,Vasiliev, L., Bayazitoglu, Y., Yener, Y., Springer Netherlands.

[4] Koo, J., & Kleinstreuer, C. (2004). Viscous dissipation effects in micro tubes and microchannels. *Int. J. Heat Mass Transfer*, **47**, 2159–2169.

[5] Cao, B., Chen, G. W., & Yuan Q. (2005). Fully developed laminar flow and heat transfer in smooth trapezoidal microchannel. *Int. Comm. Heat Mass Transfer*, **32**, 1211–1220.

[6] Morini, G. L. (2005). Viscous heating in liquid flows in micro-channels. *Int. J. Heat Mass Transfer*, **48**, 3637–3647.

[7] Kuddusi, L., & Cetegen, E. (2008). Thermal and hydrodynamic analysis of gaseous flow in trapezoidal silicon microchannels. *Int. J. Thermal Sciences*, In press.

[8] Sharipov, F. (1999). Rarefied gas flow through a long rectangular channel. *J. Vac. Sci.Technol.*, **17**(5), 3062-3066

[9] Sharipov, F. (1999). Non-isothermal gas flow through rectangular microchannels. *J. Micromech. Microeng.*, **9**, 394-401

[10] Morini, G. L. & Spiga, M. (2007). The role of the viscous dissipation in heated microchannels. *Trans. ASME*, **129**, 308–318

[11] Tao, W.Q. (2001). *Numerical Heat Transfer*, Second ed., The Xian Jiao Tong University Press, Xi An.

[12] Morini, G. L., Spiga, M., & Tartarini, P. (2004). The rarefaction effect on the friction factor of gas flow in microchannels. *Super lattices and Microstructures*, **35**, 587–599.

[13] Kuddusi, L. (2007). Prediction of temperature distribution and Nusselt

number in rectangular microchannels at wall slip condition for all versions of constant wall temperature. *Int. J. Thermal Sciences*, **46**, 998–1010.